Transport and thermodynamic evidence for a marginal Fermi-liquid state in $ZrZn_2$

Mike Sutherland,[1] R. P. Smith,[1] N. Marcano,[1,2] Y. Zou,[1] S. E. Rowley,[1,3] F. M. Grosche,[1] N. Kimura,[4] S. M. Hayden,[5] S. Takashima,[6] M. Nohara,[6] and H. Takagi[6]

[1]*Cavendish Laboratory, University of Cambridge, Cambridge CB3 0HE, United Kingdom*
[2]*Centro Universitario de la Defensa, Crta. De Huesca, E-50090 Zaragoza, Spain*
[3]*Centre for Materials and Microsystems, Fondazione Bruno Kessler, Via Sommarive 18, I-38100 Trento, Italy*
[4]*Center for Low Temperature Science, Tohoku University, Sendai, Miyagi 980-8578, Japan*
[5]*H. H. Wills Physics Laboratory, University of Bristol, Tyndall Avenue, Bristol BS8 1TL, United Kingdom*
[6]*Department of Advanced Materials Science, University of Tokyo, Kashiwa, Chiba 277-8581, Japan*

(Received 24 October 2011; revised manuscript received 14 December 2011; published 18 January 2012)

Measurements of low-temperature transport and thermodynamic properties have been used to characterize the non-Fermi-liquid state of the itinerant ferromagnet $ZrZn_2$. We observe a $T^{5/3}$ temperature dependence of the electrical resistivity at zero field, which becomes T^2-like in an applied field of 9 T. In zero field, we also measured the thermal conductivity, and we see a novel linear-in-T dependence of the difference between the thermal and electrical resistivities. Heat-capacity measurements, also at zero field, reveal an upturn in the electronic contribution at low temperatures when the phonon term is subtracted. Taken together, we argue that these properties are consistent with a marginal Fermi-liquid state, which is predicted by a mean-field model of enhanced spin fluctuations on the border of ferromagnetism in three dimensions. We compare our data to quantitative predictions and establish this model as a compelling theoretical framework for understanding $ZrZn_2$.

DOI: 10.1103/PhysRevB.85.035118 PACS number(s): 72.15.Eb, 75.40.−s, 75.50.Cc, 71.27.+a

I. INTRODUCTION

The Fermi liquid theory of the metallic state is among the most successful in physics, and decades of research have established its applicability to a wide range of systems. The fundamental starting point of this theory is the existence of long-lived fermionic quasiparticles whose effective interactions lead only to nondiffractive scattering in the zero-temperature limit and near to the Fermi surface. In recent years, however, there have been a proliferation of materials that display behavior not easily understood within the Fermi-liquid picture. These so called "non-Fermi liquids" (NFLs) encompass a variety of systems. Examples include the normal state of the high-T_c cuprates,[1] one-dimensional Tomonaga-Luttinger liquids,[2,3] paramagnetic metals near a low temperature phase transition,[4] and Kondo lattice systems.[5]

A particularly rich variety of NFL behavior is exhibited by materials in which a magnetic phase transition is observed at low temperatures (see, for instance, Ref. 6). Tuning the transition to zero temperature (a quantum critical point) yields temperature dependencies of physical properties that differ from the power laws predicted by Fermi liquid theory. Early attempts to explain NFL behavior were based on the effects of strongly enhanced low-frequency, long-wavelength spin fluctuations[7–12] (often called the self-consistent renormalization or SCR theory). In the specific case of three-dimensional materials near a ferromagnetic quantum critical point, these approaches suggest characteristic transport and thermodynamic properties. For instance, the electrical resistivity is anticipated to vary as $T^{5/3}$,[13] instead of the usual T^2 behavior expected in a Fermi liquid, and the electronic heat capacity diverges logarithmically at low temperatures, instead of the Fermi liquid linear in temperature variation.

These non-Fermi-liquid temperature dependencies are a consequence of an underlying quasiparticle scattering rate, τ^{-1}, which varies linearly with the excitation energy E of a quasiparticle near the Fermi level. This is characteristic not of a Fermi liquid, for which τ^{-1} varies as E^2, but of a marginal Fermi liquid. The study of the marginal Fermi liquid (MFL) state is compelling, as it represents the weakest breakdown of the quasiparticle picture, and thus could prove to be a gateway to understanding more exotic departures from Fermi-liquid theory.

In this paper, we examine in more detail the transport of heat and charge in $ZrZn_2$ reported in a previous work,[14] which is a metal close to a three-dimensional (3D) ferromagnetic quantum critical point. We calculate the temperature dependencies of transport properties using the SCR model, and show them to be both qualitatively and semiquantitatively in agreement with our data. In particular, we pay close attention to the difference between thermal and electrical resistivities, following the analytical framework of Paglione *et al.*[15] for clean magnetic metals. We then compare these results with new measurements of the electronic specific heat, which we argue lends further support to the validity of the SCR model in this material.

II. EXPERIMENTAL DETAILS

The intermetallic compound $ZrZn_2$ crystallizes in the C15 cubic Laves structure, and is an archetypal d-band itinerant electron ferromagnet.[16] Improved sample quality as well as reports of the possible coexistence of ferromagnetism and superconductivity[17,18] have stimulated renewed interest in this compound in recent years. The highest quality samples of $ZrZn_2$ order ferromagnetically at $T_c = 28.5$ K, and magnetization measurements reveal a small moment of $0.17\mu_B$/Zr atom in the low-temperature, low-magnetic-field limit that is well below the Curie-Weiss moment $\mu_{\text{eff}} = 1.9\mu_B$/Zr atom.[19]

The ferromagnetic transition is suppressed to zero with the application of only 20 kbar of hydrostatic pressure,[14,19] which for a d-metal system of this kind, suggests that

$ZrZn_2$ is close to a ferromagnetic quantum critical point at ambient pressure. This idea is supported by de Haas–van Alphen studies, which show significantly enhanced cyclotron effective masses, as expected in the critical regime,[20] and that longitudinal fluctuations of the local magnetisation are important.[21] Inelastic neutron scattering studies support the applicability of an SCR model, since the generalized magnetic susceptibility ($\chi_{q,\omega}$) at small wave vectors, q, and small frequencies, ω, has a structure characteristic of overdamped dissipative modes with a strongly dispersive relaxation rate.[22]

In our experiments, we measured four single-crystal samples with varying levels of impurities.[23,24] The samples were thin and platelet-shaped with typical dimensions of 2 mm × 0.5 mm × 0.2 mm. We label each crystal by its residual resistivity ρ_0 and residual resistivity ratio (RRR) defined as $\rho_{300\,\mathrm{K}}/\rho_0$. These were measured to be $\rho_0 = 0.31\ \mu\Omega$cm (RRR = 210), $\rho_0 = 0.97\ \mu\Omega$cm (RRR = 67), $\rho_0 = 2.3\ \mu\Omega$cm (RRR = 29), and $\rho_0 = 6.4\ \mu\Omega$cm (RRR = 11) and were selected to cover a range of impurity concentrations.

Each sample was spark-cut into a convenient geometry, then electropolished to remove a surface layer approximately 5 μm in depth. This step was taken to avoid surface inclusions of superconducting material, shown previously to arise from the spark cutting procedure.[18] Contacts were made in a four-wire geometry using a low-power micro-spot-welding technique,[25] yielding contact resistances that were measured to be 5 mΩ or less at low temperatures.

Resistivity measurements were performed using a standard four-terminal low-frequency ac technique in a ^{3}He cryostat and in an adiabatic demagnetisation refrigerator, with low-noise transformers to enhance the signal-to-noise level. Measurements were performed on the samples with several different excitation currents between 0.1 and 1 mA and several different heating rates to ensure reproducibility.

Thermal conductivity was measured with a two-thermometer, one-heater, steady-state technique down to $T = 0.8$ K on a ^{3}He system. The reliability of our setup was tested by measuring both heat and charge transport in silver wire, obtaining the Wiedemann-Franz law at low temperatures to within 2%. Measurements were checked using different models of Cernox thermometers and different sizes of temperature gradient in order to ensure reliability.

The heat-capacity measurements between 0.3 and 100 K were conducted in a commercial Quantum Design micro calorimeter at the University of Cantabria using a standard relaxation technique. Only the purest sample was measured ($\rho_0 = 0.31\ \mu\Omega$ cm), a thin slab-shaped crystal weighing 3 mg.

III. EXPERIMENTAL RESULTS

A. Transport data

Figure 1 shows the electrical resistivity of our samples plotted against $T^{5/3}$. We observe a non-Fermi-liquid temperature dependence of the form $\rho(T) = \rho_0 + AT^{5/3}$ between 300 mK and approximately 15 K (or higher in the cleanest samples), in agreement with that observed in recent work.[23,26] No evidence of superconductivity was observed down to 300 mK in any of our crystals.

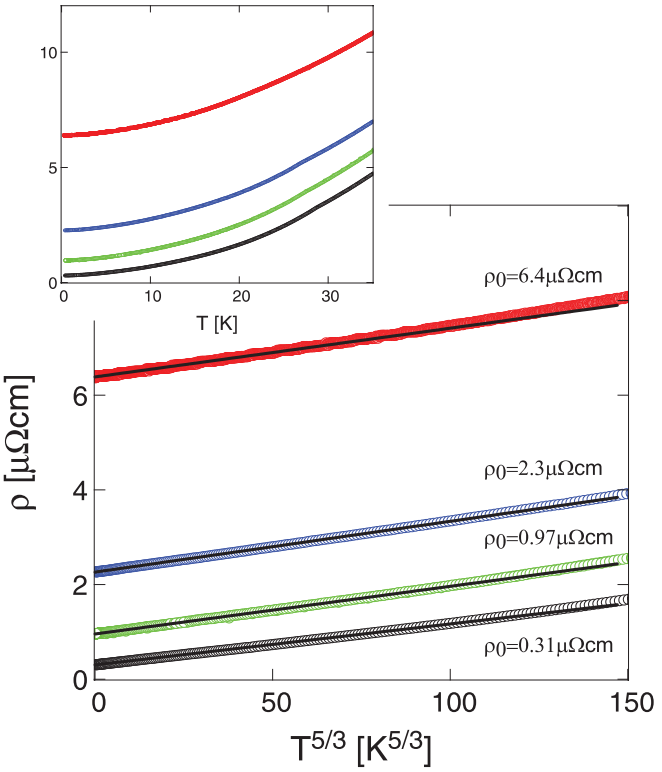

FIG. 1. (Color online) Main: Resistivity for the four samples of $ZrZn_2$ plotted against $T^{5/3}$. The straight line is a fit to the form $\rho(T) = \rho_0 + AT^{5/3}$ between 0 and 15 K. The inset shows the resistivity plotted against T for a wider temperature range.

The excellent fit to a pure $T^{5/3}$ power law indicates that the scattering of electrons by spin fluctuations is much larger than the scattering by phonons across a wide temperature range. Significant phonon scattering would normally be expected to produce a characteristic T^5 temperature dependence in the resistivity at low temperatures, crossing over to a T-linear dependence at higher temperatures. Neutron scattering measurements on $ZrZn_2$ are consistent with this observation—the observed scattering intensities are up to two orders of magnitude larger than what could be expected from phonons alone at low temperatures.[22] A similar conclusion was reached in transport studies of the cubic Laves-phase compounds RCo_2 (R = Sc,Y,Lu) by Gratz and co-workers.[27,28] In these compounds, which lie near a ferromagnetic instability and play host to spin fluctuations, it was concluded that the contribution to ρ from phonon scattering was negligible below 30 K.

Figure 2 shows how the $T^{5/3}$ state is affected by the application of a magnetic field. With $\mu_0 H = 9$ T, the resistivity recovers a characteristic Fermi-liquid-like T^2 dependence, which may be understood to arise due to the suppression or gapping of the fluctuations in a magnetic field, as suggested by measurements of the electronic specific heat.[29] The overall change in the resistivity with temperature is similarly suppressed with field, supporting this interpretation.

In can also be seen from Fig. 2 that the magnetoresistance of the sample is strongly temperature-dependent, as observed previously in polycrystalline samples.[30] At low temperatures, the effect is positive, as expected in an ordinary metal. Above $T \sim 22$ K, however, the magnetoresistance becomes negative,

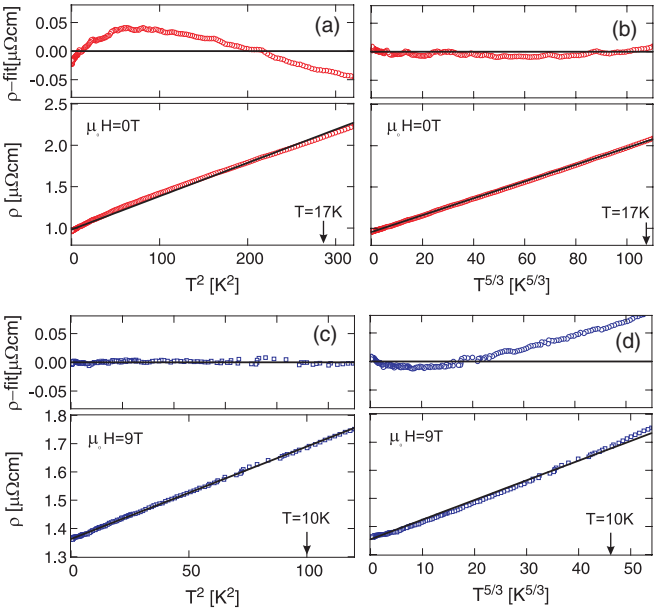

FIG. 2. (Color online) Fits to the electrical resistivity of $ZrZn_2$ (a) in zero field, fit up to 17 K as $\rho = \rho_0 + AT^2$, where A is a constant, and (b) data in zero field fit to $\rho = \rho_0 + AT^{5/3}$. Panel (c) shows the 9 T data fit up to 10 K as $\rho = \rho_0 + AT^2$, and (d) shows the 9 T data fit as $\rho = \rho_0 + AT^{5/3}$.

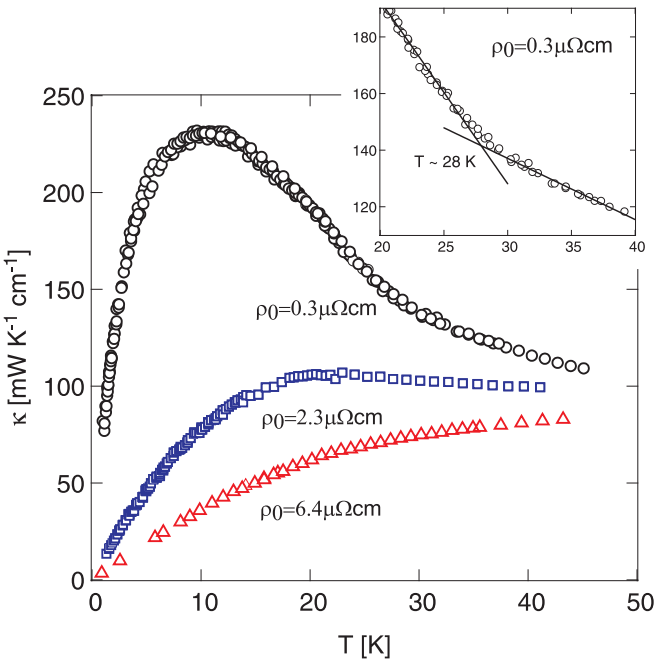

FIG. 3. (Color online) Main: Thermal conductivity of $ZrZn_2$, with samples labeled by their residual resistivities. Inset: zoom of the transition region in the cleanest sample, with $\rho_0 = 0.31\ \mu\Omega$ cm. Linear fits to the data above and below T_C suggest a change in slope occurs at $T \sim 28\ \mathrm{K} = T_c$.

suggesting that the decrease in resistivity due to the stiffening of spin fluctuations outweighs the increase in resistivity due to orbital magnetoresistance. The recovery of T^2 power law at high fields helps rule out disorder scattering as the origin of the $T^{5/3}$ power law in $\mu_0 H = 0$, since this process would have little field dependence.

Figure 3 shows the thermal conductivity of the three $ZrZn_2$ samples. In a metallic material such as $ZrZn_2$, the thermal conductivity has contributions from both electrons (κ_{el}) and phonons (κ_{ph}). In the ferromagnetic state at very low temperatures, $T \ll T_C$, we might also expect a contribution from magnons (κ_{mag}). A careful consideration of the relative magnitudes of each of these is necessary to evaluate the suitability of the MFL model in describing $ZrZn_2$.

The thermal current due to coherent, propagating magnetic modes (magnons) can be difficult to distinguish from other contributions to κ. Such modes are not the overdamped, dissipative spin excitations mentioned previously, but coherent spin waves existing at very low q that may become populated in the low-temperature regime. The contribution to thermal transport from such modes can be considerable, as was demonstrated in the antiferromagnetic insulator Nd_2CuO_4.[31,32] However, in magnetic metals κ_{mag} is limited by scattering from charge carriers,[33] which can greatly limit the conductivity. We would expect κ_{mag} to be particularly small in $ZrZn_2$ due to its very small ordered moment, which limits the phase space available for propagating magnons to $q < q_{\mathrm{sw}}$ ($q_{\mathrm{sw}} = k_\uparrow - k_\downarrow \propto M$, where $k_\uparrow$ and $k_\downarrow$ are the radii of the majority and minority spin sheets of the Fermi surface, respectively, and M is the magnetization). We thus ignore the contribution from κ_{mag}.

Between the remaining two terms, κ_{el} and κ_{ph}, we argue that by far the largest contribution to thermal conductivity at low temperatures is the electronic term, as might be expected in metals with exceptionally low ρ_0. From Fig. 3, we see that increasing the residual resistivity from 0.31 to 6.4 $\mu\Omega$ cm drastically reduces the overall thermal conductivity of the sample, and the characteristic peak seen in the cleanest sample at $T \sim 10$ K is rapidly suppressed. Since the κ_{ph} is unlikely to change much between these two samples, we can infer that the reduction in peak height is essentially due to an increase in elastic scattering of electrons from impurities. Studies of controlled levels of impurities doped into conventional ferromagnetic metals have shown a similar trend.[34]

The inset of Fig. 3 shows an expanded view of the region near the peak observed in our cleanest sample. A simple linear extrapolation above and below the kink in the data meets at $T \sim 28$ K, a reasonable estimate for the onset temperature of the peak. This is coincident with the Curie temperature $T_C = 28.5$ K,[19] and we thus attribute the peak in κ to the increase in electronic mean free path as the sample enters the ferromagnetically ordered state and spin fluctuation scattering is reduced.

A more detailed treatment of the relative magnitudes of κ_{el} and κ_{ph} lends quantitative support to our argument. We can estimate κ_{ph} by comparing data from samples with different levels of impurities as follows. We first define the thermal resistivity w using the Wiedemann-Franz law as

$$w = \frac{L_0 T}{\kappa_{\mathrm{el}}}, \tag{1}$$

where the Lorentz number $L_0 = 1/3(\pi k_B/e)^2 = 2.44\times 10^{-8}\ \mathrm{W\Omega/K^2}$. When considering the transport of both heat and charge by electrons, we must bear in mind that scattering

events may affect thermal and electrical currents in different ways. We thus define the difference between the thermal resistivity (w) and the electrical resistivity (ρ) as δ, which contains information about scattering processes:

$$\delta = w - \rho = \frac{L_0 T}{\kappa_{\rm el}} - \rho. \tag{2}$$

The difference between the effect of scattering on the charge and heat current is that while charge current is only degraded due to the quasiparticle being deflected through a scattering angle θ, the heat current is also degraded by any loss of energy ($\hbar\omega$) of the quasiparticle.[35,36] The difference between electrical and thermal resistivities can thus reveal information about the nature of inelastic scattering processes, as pointed out by Kaiser for the case of localized magnetic impurities in metallic alloys[36] and recently used to investigate antiferromagnetic fluctuations in the clean magnetic metal $CeRhIn_5$.[15] In the case of a ferromagnetic metal such as $ZrZn_2$, such inelastic processes are attributed principally to scattering from spin fluctuations.

We may now arrive at an estimate for the phonon conductivity $\kappa_{\rm ph}$. At low temperatures, in keeping with Matthiessen's rule, we assume that the amount of impurities in a given sample in the dilute limit would not considerably alter δ. In other words, we assume that the elastic and inelastic scattering channels are independent.

For two samples A and B, with differing impurity levels, we then have

$$\kappa^A = \frac{L_0 T}{\rho^A + \delta} + \kappa_{\rm ph}, \tag{3}$$

$$\kappa^B = \frac{L_0 T}{\rho^B + \delta} + \kappa_{\rm ph}. \tag{4}$$

We assume here that $\kappa_{\rm ph}$ will be the same in each sample at low temperatures, since the presence of impurities is expected to have a minimal effect on low-energy phonon modes.[37] Since we measure both κ and ρ for each sample, at every temperature we can then solve these two simultaneous equations to find both δ and $\kappa_{\rm ph}$.

The solutions of these equations for $\kappa_{\rm ph}$ are shown using the data sets from the samples with $\rho_0 = 0.31$ and 6.4 $\mu\Omega$ cm in Fig. 4. The temperature dependence of $\kappa_{\rm ph}$ below 25 K is reasonably close to the T^2 dependence typically expected from phonons scattered by electrons,[37] and a fit to this form yields a coefficient $\kappa_{\rm ph}/T^2 \sim 0.018$ mW K^{-3} cm^{-1}. Using different pairs of samples in Eqs. (3) and (4) yields almost identical curves for $\kappa_{\rm ph}$, differing in magnitude by only 20%, which demonstrates the consistency of our analysis.

The phonon contribution that we estimate using this method is seen to be rather small compared to the total conductivity of the least disorder.

Using our estimated form of $\kappa_{\rm ph}$ from Fig. 4, we now subtract this from $\kappa_{\rm tot}$ to find the electronic contribution to thermal transport. For the two samples with the lowest levels of disorder, $\kappa_{\rm ph}$ is small enough so that below $T = 15$ K, $\kappa_{\rm tot} \simeq \kappa_{\rm el}$, meaning $\kappa_{\rm el}$ is insensitive to the details of the phonon subtraction. A similar conclusion was drawn in thermal transport studies below 10 K in the very pure antiferromagnetic metal $CeRhIn_5$.[15]

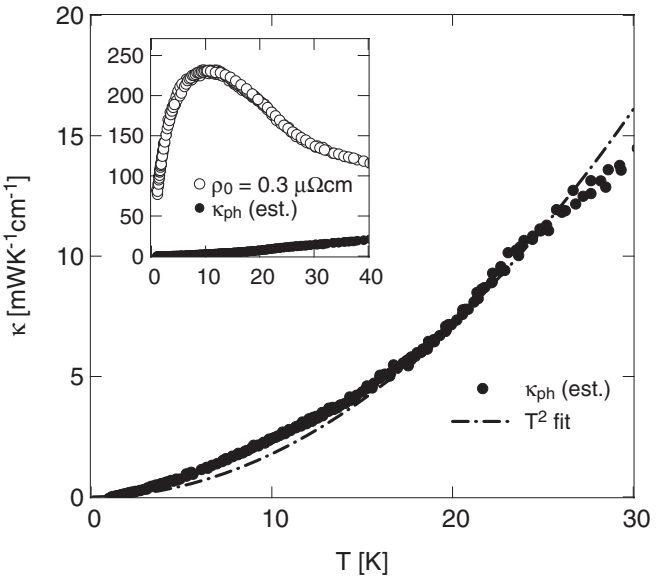

FIG. 4. The estimated phonon contribution to the total thermal conductivity using the analytical method described in the text. The dashed line represents a fit to $\kappa_{\rm ph} \propto T^2$. The inset shows the estimated phonon contribution compared to the total conductivity measured in the cleanest sample.

With the above considerations, we are in a position to study $\kappa_{\rm el}$ in isolation. In Fig. 5, we use $\kappa_{\rm el}$ to calculate the thermal resistivity w defined in Eq. (1), which we plot alongside the electrical resistivity ρ. All three samples display the same qualitative features: $w \geqslant \rho$ at finite temperatures, and $w \to \rho$ in the limit $T \to 0$ as expected from the Wiedemann-Franz law.

The difference between the two resistivities is δ, defined in Eq. (2) and plotted versus temperature in Fig. 6 for the cleanest sample. The striking linear T dependence of δ seen

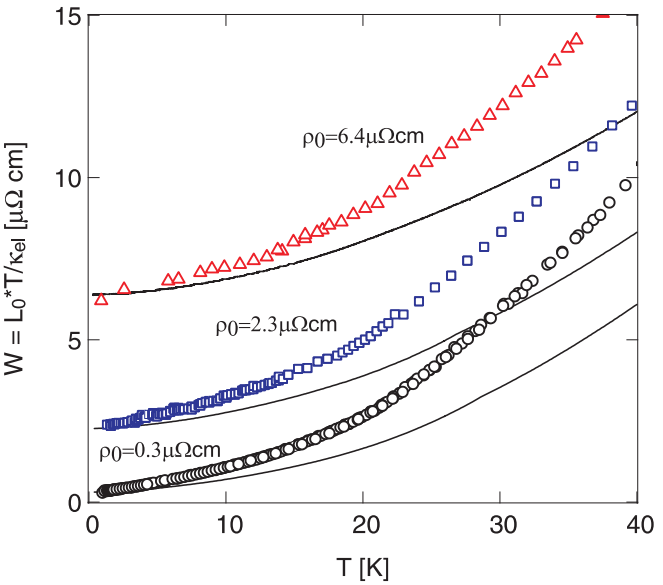

FIG. 5. (Color online) The electrical and thermal resistivity of $ZrZn_2$. The electrical resistivity data are shown as solid lines, while the thermal resistivity data are shown as data points, calculated using $w = L_0 \times T/\kappa_{\rm el}$, where $\kappa_{\rm el} = \kappa_{\rm tot} - \kappa_{\rm ph}$ as described in the text.

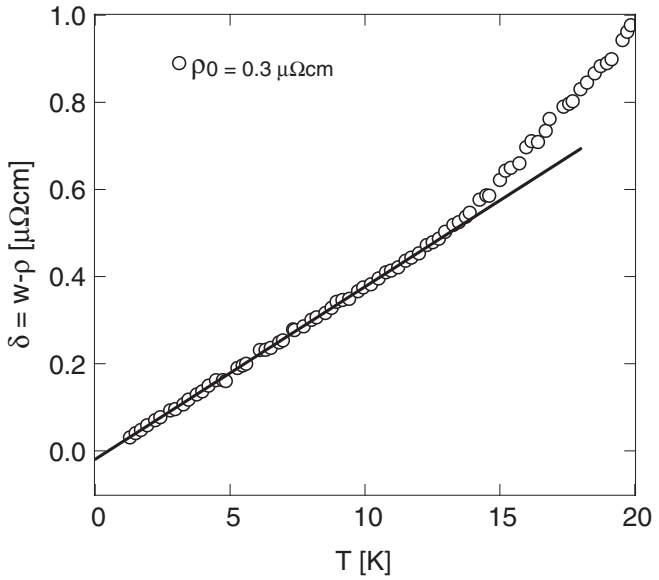

FIG. 6. The difference (δ) of the thermal ($w = L_0 T/\kappa_{el}$) and electrical (ρ) resistivities versus temperature for the sample with $\rho_0 = 0.31\ \mu\Omega$ cm. κ_{el} is found by subtracting κ_{ph} from κ_{tot}, as outlined in the text. The line is a linear fit to the data below 12 K.

in our data persists over an order of magnitude in temperature. In the usual metallic state, we would expect $\delta(T) \propto T^2$, since $w = w_0 + AT^2$ and $\rho = \rho_0 + BT^2$. The deviation from this prediction in $ZrZn_2$ is clearly related to the presence of strong inelastic scattering processes operating at low temperatures. We rule out the possibility that δ is influenced by the presence of phonon scattering at low temperatures since these processes lead to a very different behavior; in the conventional description, phonon scattering leads to a T^5 term in ρ and a T^3 term in w.[37] For $T > 12$ K, $\delta(T)$ does appear to gain some upward curvature, and we take this temperature to be the point where phonon scattering ceases to be negligible. We note that the same linear behavior is confirmed in the sample with $\rho_0 = 2.3\ \mu\Omega$ cm.

We can compare our results with those obtained in a magnetic system by Paglione *et al.*, who studied the antiferromagnetic metal $CeRhIn_5$ with $T_N = 3.8$ K.[15] In that study, δ was seen to evolve as $aT^2 + bT^5$ below the Néel temperature and dropped rapidly toward zero above. The T^5 term is due to scattering from antiferromagnetic magnons. Clearly the temperature dependence of δ at low temperatures in $ZrZn_2$ presents an interesting case—it is difficult to reconcile with either conventional electron-phonon physics or with the model used for $CeRhIn_5$. What we show in Sec. IV is that a qualitative and semiquantitative understanding of $\delta(T)$ may in fact be gained by considering scattering from spin fluctuations on the low temperature border of ferromagnetism in three dimensions. In other words, the distinct temperature dependence of $\delta(T)$ is a characteristic of the marginal Fermi-liquid state.

B. Heat capacity

The measured specific-heat capacity $C(T)$ of $ZrZn_2$ is shown in Fig. 7, and is in agreement with those reported

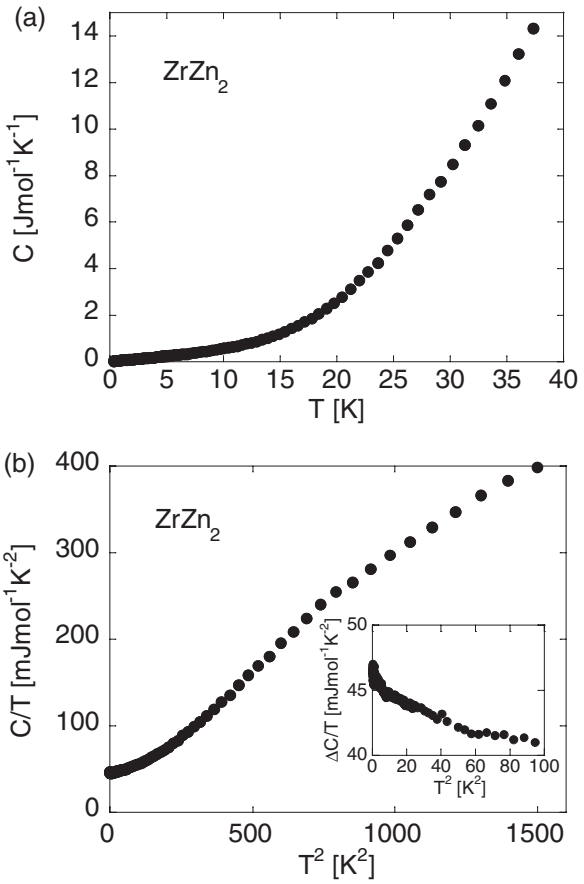

FIG. 7. (a) The heat capacity, C, of $ZrZn_2$ versus temperature, T. (b) C/T versus T^2; the inset shows $\Delta C = (C - C_{ph})/T$ vs T^2, where C_{ph} is a T^3 Debye-like phonon heat capacity whose slope is given by $\theta_D = 340$ K, as discussed in the text.

previously.[26] Figure 7(a) is a plot of C versus T and Fig. 7(b) gives C/T versus T^2. The inset of Fig. 7(b) gives $(\Delta C = C - C_{ph})/T$ versus T^2, where $C_{ph} = \beta T^3 = (12\pi^4/5)Nk_B(T/\theta_D)^3$ is the phonon contribution to the specific heat at low temperatures in which θ_D is the appropriate Debye temperature. In the plot we have taken θ_D to be 340 K,[43] a value consistent with previous estimates.[29] We show in the next section that the upturn of $\Delta C/T$ versus T^2 at low temperature is consistent, within experimental error, with the observed temperature dependences of δ and ρ and with the predictions of the SCR model with parameters relevant to $ZrZn_2$.

IV. DISCUSSION

In this section, we consider the possible description of the transport and specific-heat data in terms of the SCR model. We begin with an outline of the model and then present the predictions of the model for the model parameters that we believe are relevant to $ZrZn_2$. Finally, the results of the calculations are compared with our transport and specific-heat data.

A. Outline of the self-consistent renormalization model

The theoretical treatment of the effects of the electron-electron interactions on the transport and thermodynamic properties of nearly or weakly ferromagnetic d metals has

a long history (see, for instance, Refs. 7, 8, and 12). Here we give only an outline of the key ideas within the SCR model mentioned in the Introduction.

A discussion of transport properties in this model has been presented most notably by Ueda and Moriya.[38] In its simplest form, this model involves two isotropic bands. The carriers in one band, referred to as the s band, carry the current while the electrons in the other band, referred to as the d band, scatter the s electrons through a local s-d exchange interaction. The problem can be formulated in terms of the scattering of s electrons from the spontaneous spin fluctuations arising in the d-electron system. The spin fluctuation spectrum is characterized by a generalized dynamical and wave-vector-dependent susceptibility, which emerges as a central concept in the theory. The s electrons effectively transfer their momentum to the d electrons. It is assumed implicitly that the d electrons in turn ultimately transfer their momentum to the lattice via umklapp processes and scattering from any residual impurities present.

If we ignore residual elastic scattering due to impurities, then for $T \ll T_F$ (where T_F is the Fermi temperature for the s band), ρ and w in this model in the paramagnetic state can be written in the form

$$\left.\begin{matrix}\rho \\ w\end{matrix}\right\} = \frac{\eta}{k_B T}\sum_{q<k_c}\int_0^\infty d\omega\, n_\omega(n_\omega+1)\frac{\omega}{q}\mathrm{Im}\chi_{q,\omega}\left\{\begin{matrix}F_\rho \\ F_w\end{matrix}\right., \quad (5)$$

where n_ω is the Bose function, $n_\omega = (e^{\hbar\omega/k_B T}-1)^{-1}$, and

$$F_\rho = \left(\frac{q}{k_c}\right)^2 \quad (6)$$

$$F_w = \left(\frac{q}{k_c}\right)^2 + \left(\frac{\hbar\omega}{k_B T}\right)^2 \frac{3}{4\pi^2}\left[1-\frac{2}{3}\left(\frac{q}{k_c}\right)^2\right]. \quad (7)$$

Here η is a measure of the s-d coupling parameter, k_c is a wave-vector cutoff, equal to the diameter of the s-electron Fermi surface in the usual description, and $\chi_{q,\omega}$ is the generalized wave vector and frequency-dependent magnetic susceptibility associated with the d electrons. The factor q^2 (i.e., in F_ρ) arises from the fact that the current cannot be degraded by scattering of s electrons through an infinitesimal angle (i.e., $q \to 0$). Importantly, the factor F_w for the thermal resistivity includes a second, dynamical term, which allows for the degradation of peak current even when q is vanishingly small through strictly inelastic processes, as discussed earlier. It is this crucial term that leads to the lower-temperature exponent in w than in ρ. Note that if we set F to 1, then Eq. (5) is proportional to the quasiparticle scattering rate.

The specific heat in this model arises primarily from the d electrons, and we consider the contribution from dissipative modes.[8] In the paramagnetic state on the border of ferromagnetism at low temperature, the specific heat may be expressed within the SCR model approximately in the form

$$C = \nu T\frac{d}{dT}\sum_{q<q_c}\int_0^\infty d\omega S_\omega \mathrm{Im}\left(\frac{\partial \ln\chi_{q,\omega}}{\pi\,\partial\omega}\right), \quad (8)$$

where S_ω is the entropy of an undamped boson, i.e., a harmonic oscillator, which is given by

$$S_\omega = k_B[(1+n_\omega)\ln(1+n_\omega) - n_\omega \ln n_\omega]. \quad (9)$$

The parameters ν and q_c correspond to the degeneracy of spin fluctuation modes and the wave-vector cut-off, respectively. In the usual description, $\nu = 3$ and q_c is the diameter of the d-electron Fermi surface.

To evaluate the expressions for ρ, w, and C, we need, in particular, $\mathrm{Im}\chi_{q,\omega}$, which we model using data from inelastic neutron scattering experiments. The cut-off wave vectors k_c and q_c can be estimated from the known properties of the Fermi surface, measured in quantum oscillation experiments.[20] The parameter η can, in principle, be inferred from the Kadowaki-Woods relationship, which was shown[39] to be consistent with the SCR model under conditions in which this model reduces to the Fermi-liquid limit. Since we shall be mainly interested in the relative magnitudes of ρ and w, we shall for simplicity scale both quantities to a reference value of ρ at 15 K (a crossover temperature above which phonon contributions to the transport properties become progressively less ignorable). Although we shall focus on the relative values of ρ and w, we note that by applying the above Kadowaki-Woods relationship, we obtain in our calculations absolute values of ρ and w, which are within 20% of the measured values for the model parameters relevant to $ZrZn_2$.

Within the SCR model, $\chi_{q,\omega}$ in the paramagnetic state may be expressed in the form

$$\chi_{q,\omega}^{-1} = \chi^{-1}(T) + cq^2 - i\frac{\omega}{\gamma q}, \quad (10)$$

where $\chi(T)$ is the static magnetic susceptibility, and c and γ are constants dependent on the details of the d-electron band. The temperature dependence of the static susceptibility can, in principle, be determined self-consistently within the SCR model. Here we take $\chi(T)$ from bulk susceptibility data and the parameters c and γ from inelastic neutron scattering data, which could be satisfactorily described by the model given by Eq. (10).[22]

In the ferromagnetic state below the Curie temperature T_C, we must distinguish between the components of the spin fluctuations parallel ($\parallel$) to the ordered moment and perpendicular ($\perp$) to the ordered moment. The principal changes are as follows. First, the static susceptibility $\chi(T)$ becomes strongly dependent on the component [there are two transverse ($\perp$) components and one longitudinal ($\parallel$) component with respect to the average magnetisation.]. Secondly, the transverse component of the generalized susceptibility has a spin-wave form below the cutoff q_{sw} defined earlier. In this regime, we have[8]

$$\chi_{\perp q,\omega}^{-1} = cq^2\left(1-\omega^2/\Omega_q^2\right), \quad (11)$$

where

$$\hbar\Omega_q = Dq^2 = 2\mu_B Mcq^2 \quad (12)$$

is the spin-wave spectrum at small q.

From inelastic scattering data for $ZrZn_2$, we have approximately $\gamma = 1.8$ μeV Å and $c = 3\times10^5$ Å^2.[22] From the measured Fermi surface of $ZrZn_2$, we estimate $q_{sw} = 0.07$ Å^{-1}.[20] From bulk measurements of the magnetic equation of state, we arrive at models for $\chi_\perp(T)$ and $\chi_\parallel(T)$ as shown in Fig. 8 and $M(T) = M_0(1-T^2/T_C^2)^{1/2}$, where $M_0 = 31$ G. We note that the results of the calculations are not sensitive to precise forms of χ and M or even to the precise values of the

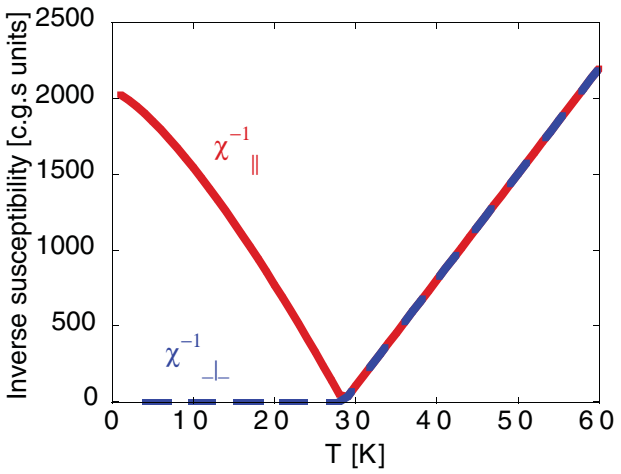

FIG. 8. (Color online) Plots showing the form of the dimensionless inverse volume susceptibility [in c.g.s units of Oe/(emu cm^{-3})] used in the resistivity calculations for $ZrZn_2$. The expressions of these are as follows: $\chi_{\parallel}^{-1} = 2\{36T_C[1-(T/T_C)^{4/3}]\}$ and $\chi_{\perp}^{-1} = 0$ for $T \leqslant T_C$ and $\chi_{\parallel}^{-1} = \chi_{\perp}^{-1} = 70(T - T_C)$ for $T > T_C$. Here we take $T_C = 28.5$ K.

other parameters. For non-Fermi-liquid behaviors to arise in this model, we require principally that χ^{-1} is small compared with cq^2 for the characteristic wave vectors for thermally excited spin fluctuations. In other words, we require that the characteristic thermal wave vector, q_T, is large compared with the magnetic correlation wave vector (i.e., the inverse of the magnetic correlation length $\xi = \sqrt{\chi/c}$).[8]

In practice, d metals such as $ZrZn_2$ cannot be represented simply in terms of two distinct species of electron as the above model suggests, and the terms "s electron" and "d electron" may not have precise meanings. It is of interest, however, to see if the model can capture some of the behaviors of ρ, w, and C, which we have measured in $ZrZn_2$.

It has been emphasized in more recent theoretical works that there should be non-analytic corrections to certain aspects of the SCR model.[40–42] Although relatively weak in three dimensions, they can nevertheless strongly modify the magnetic equation of state and in particular may give rise to a first-order ferromagnetic transition near the quantum critical point and potentially to a magnetically inhomogeneous state.[12] Therefore, we shall not attempt to calculate the magnetic equation of state self-consistently in this paper and take the temperature dependence of aspects of the magnetic equation of state from experiment. $\theta_D = 340$ K was taken from the high-magnetic-field heat-capacity data of Ref. 29.

B. The marginal Fermi-liquid limit of the SCR model

In the limit $q_T \gg \xi^{-1}$, it may be shown from Eqs. (5)–(10) that in three dimensions,

$$\rho \propto T^{5/3}, \tag{13}$$

$$\delta = (w - \rho) \propto T, \tag{14}$$

$$\tau^{-1} \propto T \ln(T^*/T), \tag{15}$$

and

$$C \propto T \ln(T^*/T), \tag{16}$$

where T^* is an appropriate temperature scale in each case separately. Note that the temperature dependence of the scattering rate τ^{-1} is different from that of δ due to the $(\omega/T)^2$ factor in Eq. (7). Thus, in this limit, the SCR model reduces to the MFL model discussed in the Introduction, while in the opposite limit, $q_T \ll \xi^{-1}$, the SCR model reduces to the FL model. For the parameters relevant to $ZrZn_2$ we find that the crossover to the FL model occurs only at temperatures below 1 K at ambient pressure.[44]

The characteristic marginal Fermi-liquid exponents for ρ and δ can be understood by analogy to the corresponding electron-phonon scattering problem. In that problem, $\rho \propto q_T^{d+2}$ and $\delta \propto q_T^d$, where d is the dimension of space. The extra factor of q_T^2 in ρ comes from the q^2 term in F_ρ [Eq. (6)] which is absent in the difference between w and δ. The temperature dependence of q_T is given by the dynamical exponent z via $T \propto q_T^z$ so that one expects

$$\rho \propto T^{\frac{d+2}{z}}, \tag{17}$$

$$\delta \propto T^{\frac{d}{z}}. \tag{18}$$

For the electron-phonon scattering problem, $z = 1$ and in 3D we recover the usual results, $\rho \propto T^5$ and $\delta \propto T^3$. For electron paramagnon scattering, however, $z = 3$ [see Eq. (10) in the limit $\chi^{-1} \to 0$] and so in 3D we expect $\rho \propto T^{5/3}$ and $\delta \propto T$ as in Eqs. (13) and (14). We caution that for dissipative modes such as paramagnons, this elementary treatment fails if z is unity or lower. In this case, ρ and δ are determined by spin fluctuations over all of q space rather than just at low q, and to obtain the FL limit of the SCR model, one must return to the full expressions for ρ and w in Eq. (5).

C. Calculations of the electrical and thermal resistivities

Using the model and parameters given above, we can calculate the electrical and thermal resistivities and the difference $\delta = w - \rho$. The results of these calculations are shown in Fig. 9 for several values of k_c (which in the model represents the typical diameter of the Fermi surface of the light electrons that principally carry the current).

The value of k_c that gives the correct magnitude of the scaled quantity $\delta(T)/\rho(15\text{ K})$ turns out to be around $k_c = 0.4$ Å^{-1}. It is interesting to note that this is close to the observed diameter of the sheet of the Fermi surface of $ZrZn_2$ with the highest characteristic Fermi velocity observed in this system. However, this fitted value of k_c should not be taken too seriously, given the complexity of the Fermi surface of $ZrZn_2$ and the relative simplicity of the present model. What seems to be significant, however, is that the calculated temperature dependences of ρ and δ are qualitatively very similar to the observed values given in Sec. III A, irrespective of the precise value chosen for k_c, or indeed of the precise values of the other model parameters.

Within the experimental temperature range of interest, we find that the SCR model reduces essentially to the MFL model, as discussed in the Introduction. In particular, ρ is predicted to vary approximately as $T^{5/3}$ and δ approximately as T in the temperature range below 15 K (above which phonon contributions become progressively more important in the measurements) and above about 1 K (well below which the SCR model predicts a Fermi liquid form for ρ and w).

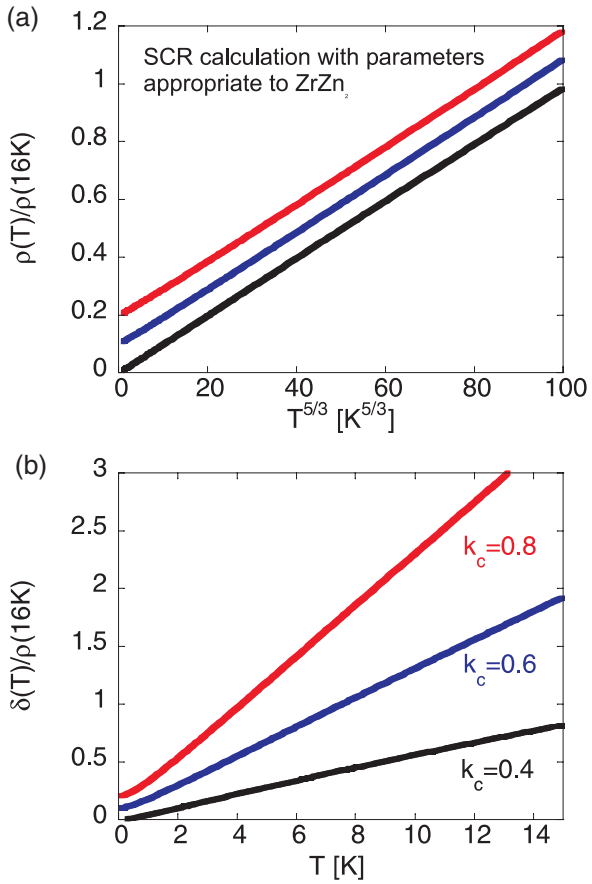

FIG. 9. (Color online) Plot showing (a) the calculated electrical resistivity plotted against $T^{5/3}$ and (b) the calculated difference between the thermal and electrical resistivities plotted against T. The results are normalized relative to the calculated electrical resistivity at 16 K. The results are shown for three values of the wave-vector cut-off parameter k_c [0.4 Å^{-1} (bottom), 0.6 Å^{-1} (middle), and 0.8 Å^{-1} (top)]. The data for $k_c = 0.6$ and 0.8 Å^{-1} are shifted upward by 0.1 and 0.2, respectively, for clarity.

D. Calculations of the specific heat

Using the model and parameters in Sec. IV A, we can also calculate the specific-heat contribution of the spin fluctuations. Below T_C, we consider the contribution from both dissipative modes and from spin waves with $q < q_{\rm sw}$. The results of the calculations are shown in Fig. 10 in the form of C/T versus T^2 for comparisons with the inset of Fig. 7(b) of the measured specific heat minus the estimated phonon contribution. The calculated heat capacity depends approximately logarithmically on the upper cut-off q_c and is also somewhat sensitive to the spin-wave cut-off $q_{\rm sw}$, although the relative contribution from the dissipative modes with $q > q_{\rm sw}$ dominates at all temperatures. The results in Fig. 10 correspond to the choice $q_c = 1$ Å^{-1}, which is approximately equal to the observed diameter of the large sheets of the Fermi surface with high effective mass (and so low Fermi velocity).

To check on the sensitivity of the result to the lower spin-wave cut-off, several values of $q_{\rm sw}$ around the value of 0.07 Å^{-1} given in Sec. IV A have been used.

Comparing the inset of Fig. 7(b) with Fig. 10, we see that the measurements are qualitatively consistent with the predictions of the SCR model, especially for a reasonable value for $q_{\rm sw}$. In particular, the upturn in C/T with decreasing temperature in the inset of Fig. 7(b) is consistent with the predictions of the SCR model. In the limit $q_T \gg \xi^{-1}$ (see Sec. IV B), this upturn is reminiscent of the logarithmic term in C expected for a marginal Fermi liquid. The magnitude of the calculated C/T is somewhat lower than the measured value. This is reasonable since the SCR model does not include the effects of the electron-phonon interaction, nor, in the form defined in Sec. IV A, the effects of any antiferromagnetic spin fluctuations that may be present.

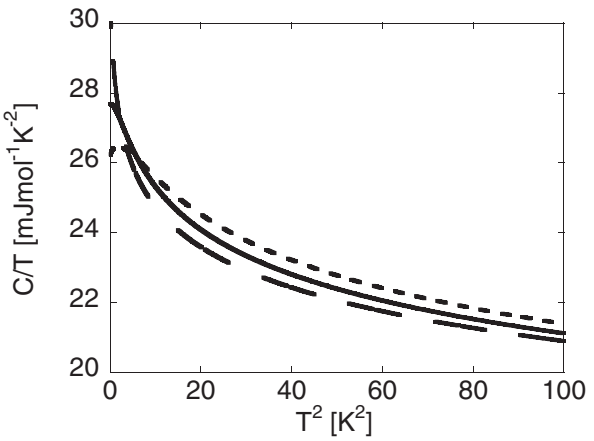

FIG. 10. Plot showing the calculated spin fluctuation heat capacity for several values of q_{sw}, namely 0.05 Å^{-1}, 0.08 Å^{-1} and 0.1 Å^{-1}. The effect of increasing q_{sw} is to cut-off the low temperature divergence of C/T.

V. CONCLUSIONS

In summary, we find that the temperature dependencies of the electrical and thermal resistivities and the electronic specific heat in $ZrZn_2$ can be understood qualitatively and even semiquantitatively in terms of the self-consistent renormalization model with model parameters inferred from independent measurements of the magnetic equation of state, the inelastic neutron scattering cross section, and the Fermi surface. Over a wide range in temperature, the SCR model reduces to the marginal Fermi-liquid model characterized by an electrical resistivity ρ varying as $T^{5/3}$, a thermal resistivity w-ρ varying as T, and a logarithmic divergence in the low-temperature specific heat. We believe that taken together, these findings provide the most compelling evidence thus far for the existence of the marginal Fermi-liquid state in the field of itinerant-electron ferromagnetism. We note that in other areas of the phase diagram, perhaps closer to the quantum critical point or at pressures beyond the critical pressure where $T_C = 0$, even more exotic departures of Fermi-liquid theory may be possible, such as those discussed in Ref. 12 and others.

ACKNOWLEDGMENTS

We thank Gil Lonzarich, Montu Saxena, Lara Sibley, and Ed Yelland for useful discussions. This work was funded by the Royal Society and EPSRC. The authors wish to thank the following organizations for financial support: R.P.S.

acknowledges St. Catherines College, University of Cambridge, N.M. acknowledges financial support from the MAT2008-06542-C04 project, S.R. acknowledges Emmanuel College Cambridge, and M.S. acknowledges the Royal Society. Special thanks go to I. R. Walker for his help in setting up the Oxford Instruments Heliox system.

[1]T. Timusk and B. Statt, Rep. Prog. Phys. **62**, 61 (1999).
[2]S. Tomonaga, Prog. Theor. Phys. **5**, 544 (1950).
[3]J. Luttinger, J. Math. Phys. **4**, 1154 (1963).
[4]N. Doiron-Leyraud, I. R. Walker, L. Taillefer, M. J. Steiner, S. R. Julian, and G. G. Lonzarich, Nature (London) **425**, 595 (2003).
[5]E. Miranda, V. Dobrosavljević, and G. Kotliar, Phys. Rev. Lett. **78**, 290 (1997).
[6]G. Stewart, Rev. Mod. Phys. **73**, 797 (2001).
[7]T. Moriya, *Spin Fluctuations in Itinerant Electron Magnetism* (Springer, Berlin, 1985).
[8]G. Lonzarich, *The Electron* (Cambridge University Press, Cambridge, 1997).
[9]J. Hertz, Phys. Rev. B **14**, 1165 (1976).
[10]A. J. Millis, Phys. Rev. B **48**, 7183 (1993).
[11]G. G. Lonzarich and L. Taillefer, J. Phys. C **18**, 4339 (1985).
[12]S. E. Rowley, R. P. Smith, N. Marcano, M. P. M. Dean, A. Kusmartseva, L. J. Spalek, E. C. T. O'Farrell, D. A. Tompsett, M. L. Sutherland, P. L. Alireza, C. Ko, C. Liu, E. Pugh, S. S. Saxena, and G. G. Lonzarich, Low. Temp. Physics **30**, 2 (2011).
[13]J. Mathon, Proc. R. Soc. London, Ser. A **306**, 355 (1968).
[14]R. Smith, M. Sutherland, G. G. Lonzarich, S. S. Saxena, N. Kimura, S. Takashima, M. Nohara, and H. Takagi, Nature (London) **455**, 1220 (2008).
[15]J. Paglione, M. A. Tanatar, D. G. Hawthorn, R. W. Hill, F. Ronning, M. Sutherland, L. Taillefer, C. Petrovic, and P. C. Canfield, Phys. Rev. Lett. **94**, 216602 (2005).
[16]E. Wohlfarth, J. Appl. Phys. **39**, 1061 (1968).
[17]C. Pfleiderer, M. Uhlarz, S. M. Hayden, R. Vollmer, H. v. Löhneysen, N. R. Bernhoeft, and G. G. Lonzarich, Nature (London) **412**, 58 (2001).
[18]E. A. Yelland *et al.*, Phys. Rev. B **72**, 214523 (2005).
[19]M. Uhlarz, C. Pfleiderer, H. v. Löhneysen, S. Hayden, and G. Lonzarich, Physica B **312**, 487 (2002).
[20]S. J. C. Yates, G. Santi, S. M. Hayden, P. J. Meeson, and S. B. Dugdale, Phys. Rev. Lett. **90**, 057003 (2003).
[21]E. A. Yelland and S. M. Hayden, Phys. Rev. Lett. **99**, 196405 (2007).
[22]G. G. Lonzarich, N. R. Bernhoeft, and D. M. Paul, Physica B **156-157**, 699 (1989).
[23]S. Takashima, M. Nohara, H. Ueda, N. Takeshita, C. Terakura, F. Sakai, and H. Takagi, J. Phys. Soc. Jpn. **76**, 043704 (2007).
[24]N. Kimura, M. Endo, T. Isshiki, S. Minagawa, A. Ochiai, H. Aoki, T. Terashima, S. Uji, T. Matsumoto, and G.G. Lonzarich,Phys. Rev. Lett. **92**, 197002 (2004).
[25]I. Walker and C. Moss, Rev. Sci. Instrum. **69**, 2747 (1998).
[26]E. A. Yelland, S. J. C. Yates, O. Taylor, A. Griffiths, S. M. Hayden, and A. Carrington, Phys. Rev. B **72**, 184436 (2005).
[27]E. Gratz, Physica B **237**, 470 (1997).
[28]E. Gratz and A. Markosyan, J. Phys. Condens. Matter **13**, R385 (2001).
[29]C. Pfleiderer, A. Faisst, H. v Lohneysen, S. M. Hayden, and G. G. Lonzarich, J. Magn. Magn. Mater. **226-230**, 258 (2001).
[30]S. Ogawa, Physica B **91**, 82 (1977).
[31]S. Y. Li, L. Taillefer, C. H. Wang, and X. H. Chen, Phys. Rev. Lett. **95**, 156603 (2005).
[32]Z. Y. Zhao, X. M. Wang, B. Ni, Q. J. Li, C. Fan, W. P. Ke, W. Tao, L. M. Chen, X. Zhao, and X. F. Sun, Phys. Rev. B **83**, 174518 (2011).
[33]W. B. Yelon and L. Berger, Phys. Rev. Lett. **25**, 1207 (1970).
[34]T. Farrell and D. Grieg, J. Phys. C **2**, 1465 (1969).
[35]J. Schriempf and A. Schindler, Phys. Rev. **187**, 959 (1969).
[36]A. Kaiser, Phys. Rev. B **3**, 3040 (1971).
[37]J. M. Ziman, *Electrons and Phonons* (Clarendon, Oxford, England, 1960).
[38]K. Ueda and T. Moriya, JPSJ **39**, 605 (1975).
[39]T. Moriya and T. Takimoto, J. Phys. Soc. Jpn. **64**, 960 (1995).
[40]D. Belitz, T. R. Kirkpatrick, and T. Vojta, Phys. Rev. B **55**, 9452 (1997).
[41]G. Y. Chitov and A. J. Millis, Phys. Rev. B **64**, 054414 (2001).
[42]A. V. Chubukov, D. L. Maslov, and A. J. Millis, Phys. Rev. B **73**, 045128 (2006).
[43]$\theta_D = 340$ K was taken from the high-magnetic-field heat-capacity data of Ref. 29. At high field, the effect of spin fluctuations is suppressed and the Fermi-liquid form $C/T = \text{const}$ should be recovered while the field should not significantly affect the phonon heat capacity. This allows θ_D to be extracted from a fit of C/T versus T^2 over the required temperature range of 0–10 K.
[44]This should be contrasted with the analogous problem in MnSi, where in the same model, but with parameters relevant to MnSi, the FL crossover temperature is an order of magnitude higher. In MnSi, the MFL regime is squeezed out by the FL domain at low temperatures and the phonon contribution at higher temperatures. In $ZrZn_2$, the MFL is then expected to be a good approximation to the SCR model over a wide temperature range, up to over 50 K (with the exception of a narrow region close to T_C) if the phonon contributions can be ignored. The phonon contribution ignored in the SCR model in practice limits the applicability of the MFL to below about 15 K in $ZrZn_2$.